

Leaching kinetics of low-grade copper ore containing calcium-magnesium carbonate in ammonia-ammonium sulfate solution with persulfate

LIU Zhi-xiong^{1,2}, YIN Zhou-lan¹, HU Hui-ping¹, CHEN Qi-yuan¹

1. School of Chemistry and Chemical Engineering, Central South University, Changsha 410083, China;
2. College of Chemistry and Chemical Engineering, Jishou University, Jishou 416000, China

Received 30 September 2011; accepted 23 December 2011

Abstract: The leaching kinetics of copper from low-grade copper ore was investigated in ammonia-ammonium sulfate solution with sodium persulfate. The effect parameters of stirring speed, temperature, particle size, concentrations of ammonia, ammonium sulfate and sodium persulfate were determined. The results show that the leaching rate is nearly independent of agitation above 300 r/min and increases with the increase of temperature, concentrations of ammonia, ammonium sulfate and sodium persulfate. The EDS analysis and phase quantitative analysis of the residues indicate that bornite can be dissolved by persulfate oxidization. The leaching kinetics with activation energy of 22.91 kJ/mol was analyzed by using a new shrinking core model (SCM) in which both the interfacial transfer and diffusion across the product layer affect the leaching rate. A semi-empirical rate equation was obtained to describe the leaching process and the empirical reaction orders with respect to the concentrations of ammonia, ammonium sulfate and sodium persulfate are 0.5, 1.2 and 0.5, respectively.

Key words: low-grade copper ore; calcium-magnesium carbonate; leaching kinetics; ammoniacal solution; sodium persulfate; activation energy; shrinking core model

1 Introduction

Copper ore exists mainly in the forms of sulfide and oxidized copper ore, such as chalcopyrite, bornite, malachite and chrysocolla. Copper sulfides are generally separated and concentrated from gangue by flotation and treated by conventional pyrometallurgical processes. Although treatments by pyrometallurgical processes are not attractive on account of large amounts of SO₂ produced, approximately 80%–85% of the total metallic copper is produced pyrometallurgically [1]. However, with gradual depletion of high-grade copper ore deposits, it becomes more difficult to extract copper by the conventional pyrometallurgical methods. Hydrometallurgy is suitable for lean and complex ores, especially low-grade ores, waste rocks tailings [2–4], and results in the increase of metal recoveries and the reduction of air pollution hazard.

There are many studies related to the leaching of oxidized and sulfide copper ores in ammoniacal media [5–13] or acidic media [14–16]. If there is a preponderance of carbonates or siliceous gangue in the

ore, acid medium is not suitable for leaching owing to the excessive acid consumption. However, ammonia is an attractive reagent because it does not react with carbonates and siliceous gangue, and then it is ease of purification, low-cost production and amenability to regeneration.

The dissolution of covellite was investigated in ammoniacal solutions under the oxygen pressure conditions [17]. It was found that the dissolution kinetics was controlled by chemical reaction rate. The ammonia-oxygen leaching of chalcopyrite in an in-situ environment was performed by BELL et al [18]. It could be concluded that the most significant parameters for chalcopyrite in ammoniacal lixivants were temperature, oxygen pressure and ammonia concentration. Activation energies were 31.4 kJ/mol and 37.7 kJ/mol for two different chalcopyrite specimens. EKMEKYAPAR et al [19] studied the dissolution kinetics of an oxidized copper ore containing malachite mainly and covellite slightly in water saturated by chlorine. It was found that the dissolution proceeded in two stages and was controlled by diffusion through the ash layer in each stage. The dissolution kinetics of copper ore were

$1-3(1-x)^{2/3}-2(1-x)=k_1t$ and $1-3(1-x)^{2/3}-2(1-x)=k_2t$ (where x is reaction fraction, k_1 and k_2 are rate constants, t is time) for the first and second stages, respectively. The activation energies were 27.15 kJ/mol (I) and 20.21 kJ/mol (II), respectively.

Tangdan oxidized copper ore, which contains high-grade calcium magnesium carbonate gangues and has poor floatable characteristics, is one of the largest copper mines in China. Its reserve is about 115×10^4 t and its average content of copper is 0.75% (mass fraction). LIU et al [12] investigated the dissolution kinetics of low-grade copper ore in ammonia-ammonium chloride solution. The results indicate that the malachite is dissolved easily and chrysocolla is extracted difficultly in ammoniacal solution and bornite is not dissolved in ammonia leaching without oxidants. Therefore, it makes a focus that how to extract bornite in ammoniacal solution.

Persulfate is known to be a strong oxidant in the basic solutions and has been used as a leaching agent for the recovery of metal in alkaline solutions [20,21]. The dissolution of low-grade copper ore in ammonia-ammonium sulfate solution with persulfate has not been reported.

In the present study, the effects of concentrations of ammonia, ammonium sulfate and sodium persulfate, temperature, particle size and stirring speed on the leaching rate of low-grade copper ore in ammonia-ammonium sulfate solution are interpreted.

2 Experimental

2.1 Materials

The oxidized copper ore from Yunnan province in China was ground into different particle sizes of 0.037, 0.045–0.063, 0.074–0.100, 0.150–0.180, 0.250–0.300 mm. The chemical analysis and X-ray diffraction pattern of the copper ore are given in Table 1 and Fig. 1, respectively. The content of copper in the ore is too low to be detected by X-ray diffraction method. Figure 1 indicates that gangue contains muscovite, calcite, dolomite and quartz.

Table 1 Chemical composition of oxidized copper ore (mass fraction, %)

CuO	CaO	MgO	SiO ₂	Fe ₂ O ₃	ZnO	Al ₂ O ₃	K ₂ O	Na ₂ O
0.96	29.00	12.92	25.90	2.84	0.11	1.95	1.35	0.07

The SEM images and corresponding EDS analyses, the mineralogical composition and the element analysis of EDS for the oxidized copper ore with particle size of 0.045–0.063 mm are presented in Fig. 2, Table 2 and

Table 3, respectively. The phases of copper in the ore were identified to be malachite mainly, chrysocolla secondly and bornite thirdly, corresponding to free copper oxide, copper silicate and second copper sulfide (Table 2). The analysis results of element contents by EDS in Table 3 are very close to the theoretical values of malachite, chrysocolla and bornite, respectively. Hence, the phases of copper deduced by EDS analysis are the same as those observed by the polarizing microscope method.

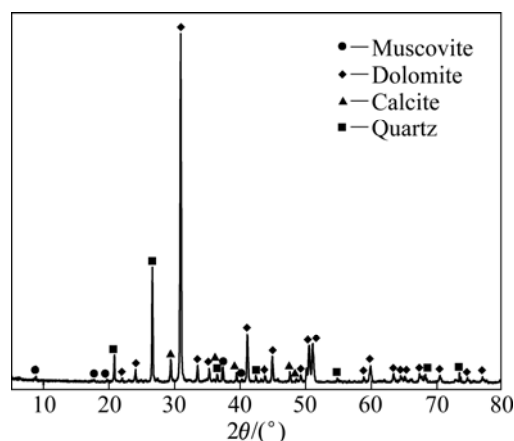


Fig. 1 X-ray diffraction pattern of copper ore

Table 2 Phase composition of oxide copper ore

Phase	w(Cu)/%	Relative content of Cu /%
Free copper oxide	0.383	49.74
Copper silicates	0.220	28.57
Second copper sulfide	0.160	20.78
Primary copper sulfide	0.007	0.91
Total Cu	0.770	100.00

Table 3 Element content of copper ore by EDS (mass fraction %)

Area in Fig. 2	Cu	Fe	S	O	Si	Ca	Mg	C	Cl
Area 1	59.89	0.96		29.00	3.89	1.08		5.18	
Area 2	45.13	1.60		30.92	21.43	0.71		0.21	
Area 3	60.13	10.11	22.08		1.22	1.40	2.94		1.22

2.2 Leaching procedure

The leaching experiments were performed in a 500 mL reactor with a four-neck split flask in a thermostatic heating mantle. The reactor was equipped with a condenser, a mercury thermometer, an overhead mechanical stirrer and a rubber stopper to take samples from the leaching solution. The desired temperature of the flask within ± 0.5 °C was adjusted by a thermostatically controlled electric heating mantle. Agitation was provided by a mechanical stirrer. 200 mL

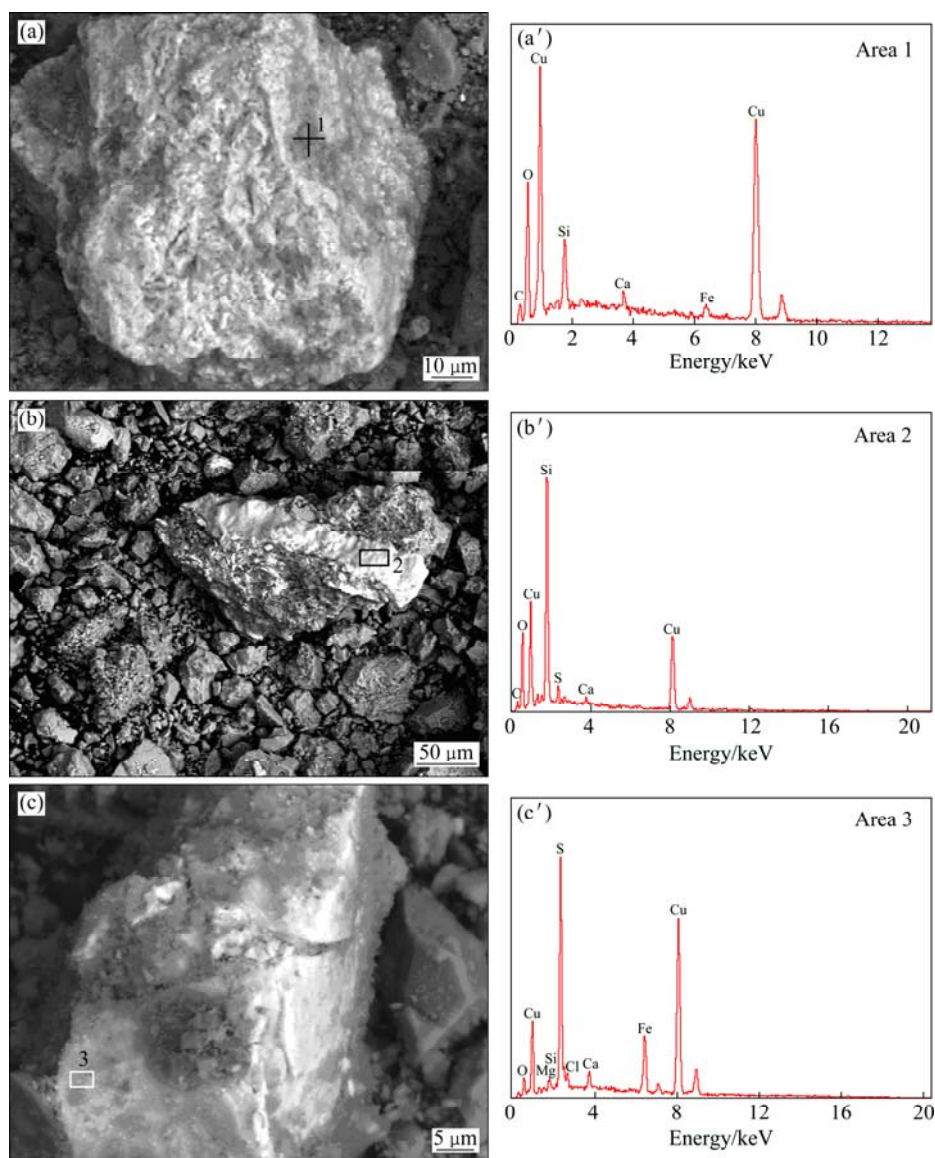


Fig. 2 SEM images (a,b,c) and corresponding EDS analyses (a',b',c') of copper ore (White parts contain copper minerals)

solution containing specific lixiviant was added into the reactor. When the desired stirring speed and reaction temperature were reached, the solid sample was added into the reactor. 2 mL of sample solution was withdrawn at specific time intervals and filtered for analyzing the concentration of copper by an atomic absorption spectrophotometer (AAS). At the same time, 2 mL of fresh lixiviant was added into the reactor to keep the volume of the solution constant. Filtration was made after each leaching experiment. The leached residue was weighed after being dried at 110 °C for 8 h.

3 Results and discussion

The effect of agitation speed on the copper leaching was carried out in the range from 100 to 500 r/min. An adequate suspension of the solid was observed at 300

r/min and the copper dissolution was independent of the agitation over this speed. As a result, agitation speed was maintained at 500 r/min in the subsequent experiments to eliminate the effect of agitation as a variable on the leaching rate.

3.1 Effect of temperature

The effect of temperature on the dissolution of copper was investigated in the range from 293 to 323 K. The results are given in Fig. 3. It can be observed that the extraction of copper increases with the increase of leaching time at different temperatures. The copper dissolution rate is greatly affected by temperature. When the temperature ranges from 293 to 323 K, the extraction of copper is increased from 30.2% to 50.1% after 2 min. The extraction of copper after 60 min reaches 80 % at 293 K and 89.4 % at 323K, respectively.

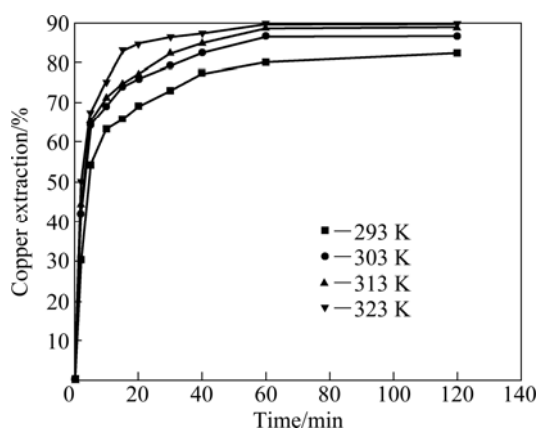


Fig. 3 Effect of temperature on extraction of copper (2.5 mol/L ammonia, 2.0 mol/L ammonium sulfate, 0.05 mol/L sodium persulfate, stirring speed 500 r/min, liquid-to-solid ratio 40 mL/g and particle size 0.045–0.063 mm)

3.2 Effect of ammonia and ammonium sulfate concentration

Experiments on the dissolution of the copper ore were performed to investigate the effect of ammonia concentration at 2.0 mol/L ammonium sulfate. The results are shown in Fig. 4(a). It is indicated that the

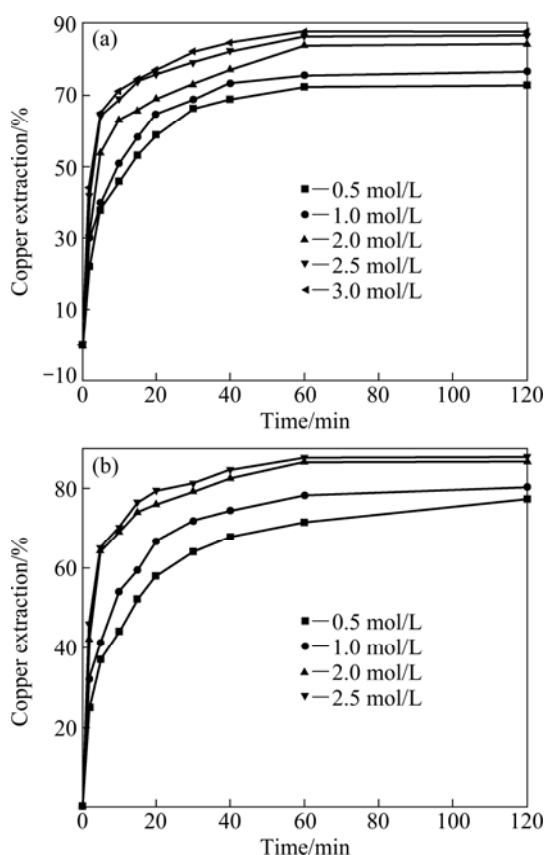


Fig. 4 Effect of concentrations of ammonia (a) and ammonium sulfate (b) on extraction of copper (Temperature 303 K, 0.05 mol/L sodium persulfate, stirring speed 500 r/min, liquid-to-solid ratio 40 mL/g and particle size 0.045–0.063 mm)

extraction of copper increases with the increase of ammonia concentration when more reaction molecules can attack the solid.

The effect of ammonium sulfate concentration on the dissolution of copper was investigated at 2.5 mol/L ammonia as shown in Fig. 4(b). It illustrates that the leaching rate increases when the concentration of ammonium sulfate increases.

3.3 Effect of sodium persulfate concentration

Figure 5 shows the effect of sodium persulfate concentration on the leaching rate of copper at 303 K. It shows that the extraction of copper increases with the increase of sodium persulfate concentration in the range assessed. At the initial time of leaching, the extraction of copper increases greatly. The extraction of copper reaches 86.2% and 87.6% when the concentrations of persulfate are 0.050 and 0.075 mol/L at 60 min, respectively. And then there is no significant increase for the extraction of copper.

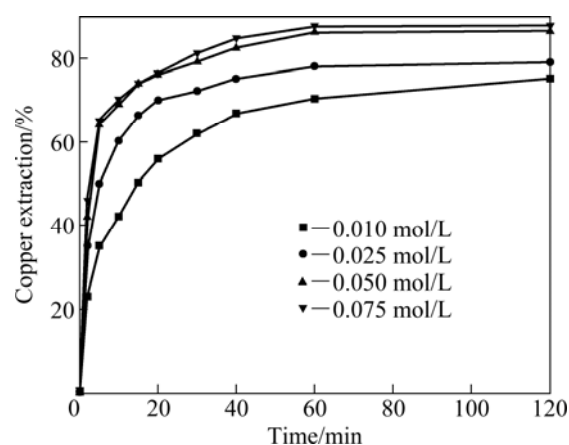


Fig. 5 Effect of sodium persulfate concentration on extraction of copper (Temperature 303K, 2.5 mol/L ammonia, 2.0 mol/L ammonium sulfate, stirring speed 500 r/min, liquid-to-solid ratio 40 mL/g and particle size 0.045–0.063 mm)

3.4 Effect of particle size

Experiments were performed to investigate the effects of particle sizes on the dissolution behavior of copper. The results are presented in Fig. 6. As expected, the smaller the size of the particles, the faster the dissolution rate. It is possibly attributed to the active sites of the copper ores on the surface of particles in the dissolution. When the specific size gets smaller, more active sites on the solid surface are exposed to the solution. As the leaching proceeds, the reactants penetrate into the micro-cracks and more soluble forms of copper are extracted.

3.5 Effect of liquid-to-solid ratio

The effect of liquid-to-solid ratio range on the

leaching of low grade oxidized copper ore was investigated from 10 to 50 mL/g at 303 K. The results are given in Fig. 7. It indicates that the increase of liquid-to-solid ratio can enhance the leaching of copper. But there is no significant change on the extraction of copper when liquid-to-solid ratio increases. This can be explained that the lixiviant is excess of the calculated amount for the extraction of copper.

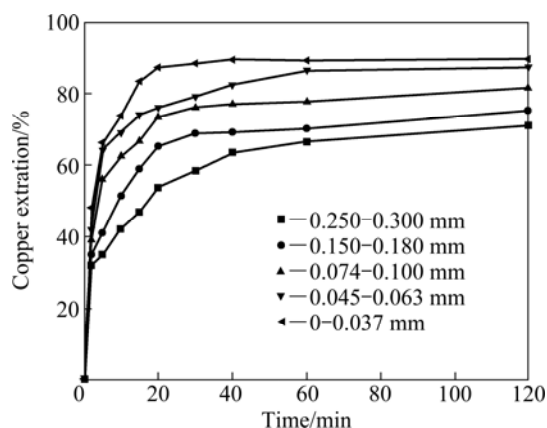


Fig. 6 Effect of particle size on extraction of copper (Temperature 303 K, 2.5 mol/L ammonia, 2.0 mol/L ammonium sulfate, 0.05 mol/L sodium persulfate, liquid-to-solid ratio 40 mL/g, stirring speed 500 r/min)

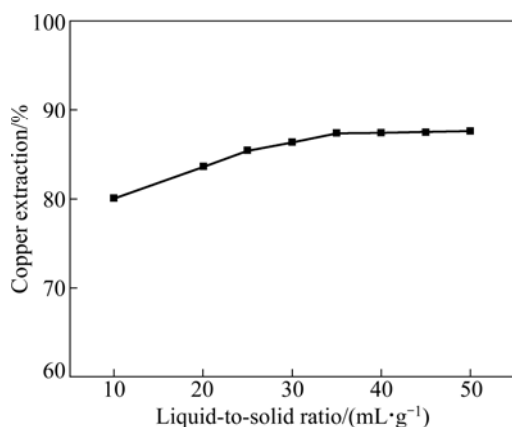
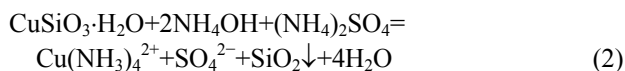
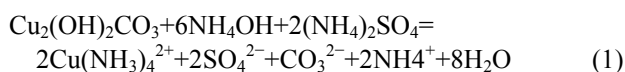


Fig. 7 Effect of liquid-to-solid ratio on extraction of copper (Temperature 303 K, 2.5 mol/L ammonia, 2.0 mol/L ammonium sulfate, 0.05 mol/L sodium persulfate, leaching time 120 min, stirring speed 500 r/min, and particle size 0.045–0.063 mm)

3.6 Dissolution mechanism and residue analysis

Malachite and chrysocolla in ammoniacal solution take place according to Eq. (1) and Eq. (2), respectively:



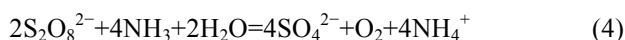
PARK et al [22] and REILLY and SCOTT [17] drew the similar conclusion that S^{2-} in the sulphide minerals is eventually oxidized into SO_4^{2-} in

ammonia-oxygen solution.

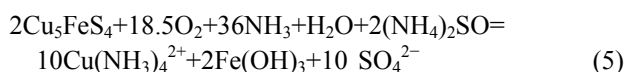
FURMAN et al [23] proposed the decomposition mechanism of persulfate in alkaline solution as follows:



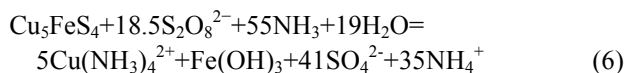
Equation (3) indicates that the reaction of $\text{S}_2\text{O}_8^{2-}$ with ammonia may take place as follows:



The dissolution of bornite in ammonia-oxygen system may occur according to the following reaction:



Summing reactions Eq. (4) and Eq. (5) provides the following net reaction for the leaching of bornite in ammonia-ammonium sulfate with persulfate:



Equation (1) indicates that malachite can be dissolved, Eq. (2) indicates that chrysocolla may be dissolved difficultly owing to the absorption of silica on the surface of the solid, and Eq. (3) indicates that bornite may be dissolved by oxidation of persulfate.

The SEM images of the leaching residues and the element analysis of the EDS are shown in Fig. 8 and Table 4, respectively. The micrographs of the solid particles before leaching present a rough and porous surface as observed in Fig. 2. However, the micrographs of the leaching residues present different surfaces. Malachite was almost dissolved and could not be observed in the leaching residue by EDS. Figure 8(a') and Table 4 indicate that chrysocolla is dissolved partly compared with Fig. 2(b'). Figure 8(a) shows that the morphology of the undissolved and partially dissolved chrysocolla is a little bit more rough and porous than that of chrysocolla before leaching (Fig. 2(b)). During the leaching, the precipitated silica is absorbed on the surface of the particle of chrysocolla as observed in Fig. 8(a), which may block the surface-active sites of the copper ores and reduce the reactivity. Figure 8(b') shows that bornite can be mostly oxidized with persulfate compared with Fig. 2(c'). As seen from Fig 8(b), the morphology of the residue derived from the oxidation of bornite is different from that of the ore before leaching and presents a rough and porous surface which is of needle-shape to a certain extent. The phases of copper in the ore before and after leaching are listed in Table 5. It confirms that bornite can be oxidized and dissolved by persulfate in the ammonia-ammonium sulfate solution.

3.7 Kinetics analysis

The shrinking core model (SCM) considers that the rate of controlling step of dissolution process is either the

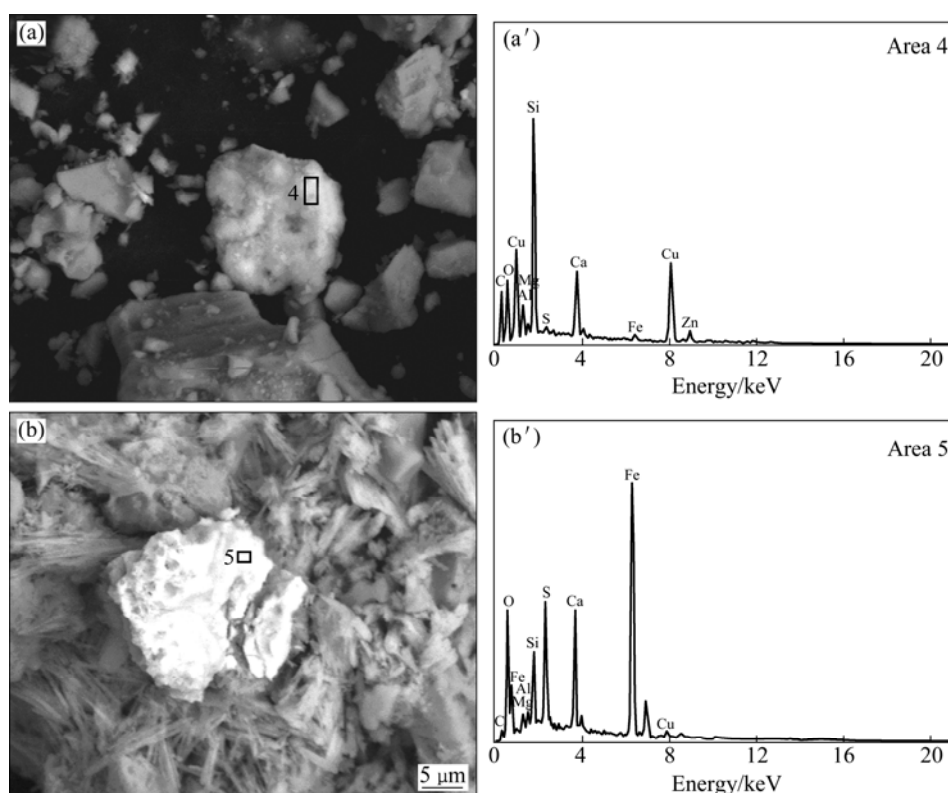


Fig. 8 SEM images (a,b) and EDS analyses (a',b') of leaching residue (The white parts contain copper minerals)

Table 4 EDS analysis for leaching residue (mass fraction %)

Area	Cu	Fe	S	O	Si	Ca	Mg	C	Al
4	32.08	1.37	0.54	23.43	14.51	4.96	2.82	17.96	0.59
5	2.63	49.80	8.07	7.48	3.86	8.07	1.57		0.67

Table 5 Phase of copper in copper ore before and after leaching

Phase	w(Cu)/%		Relative content of Cu /%	
	Before leaching	After leaching	Before leaching	After leaching
Free copper oxide	0.383		49.74	
Copper silicates	0.220	0.101	28.57	93.52
Second copper sulfide	0.007	0.003	0.91	2.78
Primary copper sulfide	0.160	0.004	20.78	3.70
Total Cu	0.770	0.108	100	100

diffusion through solution boundary, or the diffusion through a solid product layer, or the surface chemical reaction. Assuming that the copper particles have a spherical geometry and the process is controlled by diffusion through production layer, the integrated equation of the shrinking core model can be expressed as [24]

$$1-(2/3)x-(1-x)^{2/3}=k_d t \quad (7)$$

When the process is chemically controlled, the

integrated equation of the shrinking core model can be given as [24]

$$1-(1-x)^{1/3}=k_r t \quad (8)$$

where x is reaction fraction, k_d and k_r are rate constants, and t is reaction time.

According to Eq. (7) and Eq. (8), when the process is controlled by diffusion through a solid product layer, the plot of $1-(2/3)x-(1-x)^{2/3}$ versus time is a straight line with a slope k_d , similarly, when the process is chemically controlled, the plot of $1-(1-x)^{1/3}$ versus time is also a straight line with a slope k_r . Equations (7) and (8) are often used to describe the leaching process when it is controlled by diffusion through a solid product layer or by chemical reaction.

For the kinetics analysis in the present work, the shrinking core models with diffusion through product layer and surface chemical reaction, Eq. (7) and Eq. (8) were evaluated. The left sides of these expressions were plotted with respect to the leaching time, and then the correlation of the kinetics data with these models was assessed by using correlation coefficient (R^2) values in Table 6. The slopes of these plots are the apparent rate constants (k_d and k_r).

Although the dissolution-controlled model Eq. (7) fitted better compared with the chemically controlled model Eq. (8), the SCM with diffusion-controlling is not well fitted with the experimental data. The correlation

coefficients (R^2) for diffusion control and chemical control were both below 0.84. Hence, a new SCM proposed by DICKINSON and HEAL [25] was applied to describing the dissolution process. This model is based on the assumption that both the interface transfer and diffusion across the product layer affect the leaching rate. Equation of this model is written as follows:

$$(1/3)\ln(1-x)+(1-x)^{-1/3}-1=kt \quad (9)$$

The results of the kinetics analysis including the correlation coefficient when the leaching data were fitted to Eq. (9) are shown in Table 6. As can be seen from Table 6, the model Eq. (9) fits the best in all the experiments. Therefore, model of Eq. (9) was adopted to describe the dissolution of copper in ammonia-ammonium sulfate solution with persulfate. Figure 9 presents a good fit ($R^2 > 0.9455$) by plotting $(1/3)\ln(1-x)+(1-x)^{-1/3}-1$ versus time at different temperatures.

Table 6 Correlation coefficients (R^2) of three kinetics models at different temperatures

T/K	R^2		
	$1-(1-x)^{1/3}$	$1-(2/3)x-(1-x)^{2/3}$	$(1/3)\ln(1-x)+(1-x)^{-1/3}-1$
293	0.6258	0.8017	0.9455
303	0.5939	0.7769	0.9475
313	0.6645	0.8301	0.9736
323	0.5694	0.7395	0.9468

The Arrhenius plot constructed with the rate constant value (k), which is calculated from the data given in Fig. 9, is presented in Fig. 10. The calculated activation energy (E_a) for the dissolution of the oxidized copper ore is 22.91 kJ/mol.

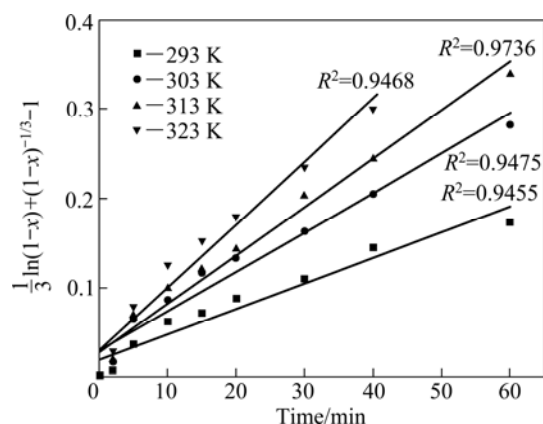


Fig. 9 Plots of $(1/3)\ln(1-x)+(1-x)^{-1/3}-1$ versus time at different temperatures

A serious well-fitted plots of $(1/3)\ln(1-x)+(1-x)^{-1/3}-1$ versus time at different concentrations of ammonia, ammonium sulfate and sodium persulfate are given in Fig. 11. From the slopes of the straight lines in

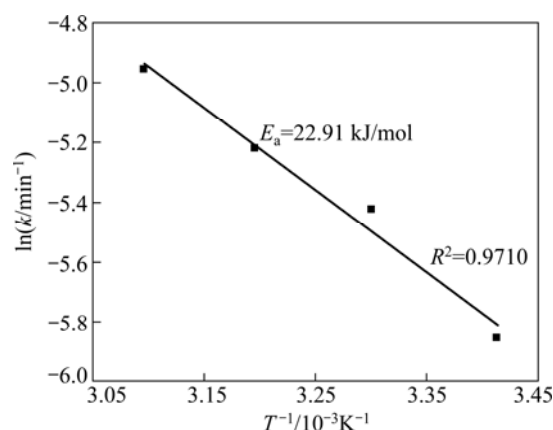


Fig. 10 Arrhenius plot of copper dissolution of oxidized copper ore

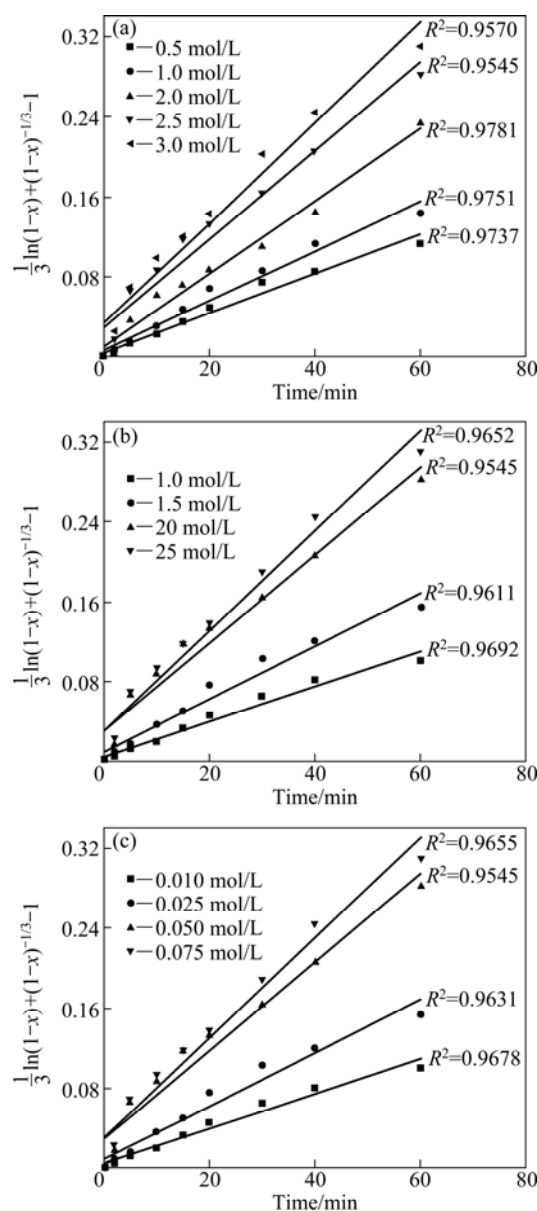


Fig. 11 Plots of $(1/3)\ln(1-x)+(1-x)^{-1/3}-1$ versus time at different concentrations of ammonia, ammonium sulfate and sodium persulfate

Fig. 11(a), the apparent rate constant (k) was determined and $\ln k$ versus $\ln[\text{NH}_3\text{H}_2\text{O}]$ plot (Fig. 12(a)) was constructed to determine the order of dependency with respect to ammonia concentration. The empirical reaction order for ammonia concentration is 0.5. In a similar way, the empirical reaction orders obtained for ammonium sulfate and sodium persulfate concentrations are 1.2 and 0.5, respectively (Fig. 12).

The control parameters used in the present work, including temperature, concentrations of ammonia,

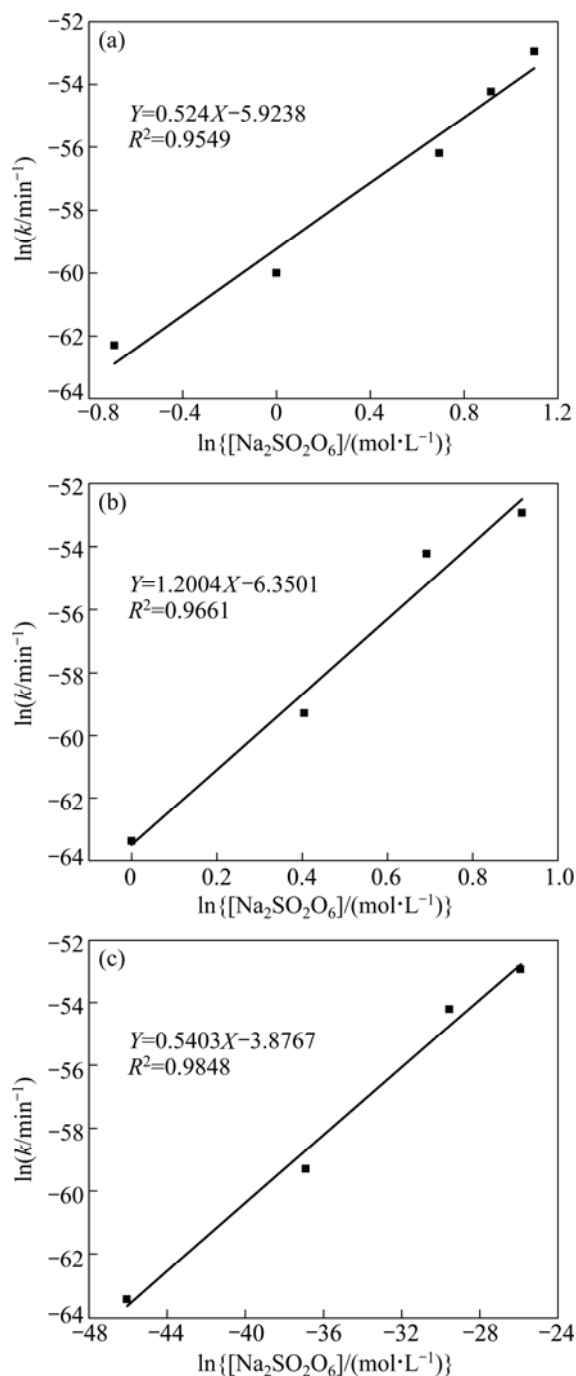


Fig. 12 Plots of $\ln\{d[(1/3)\ln(1-x)+(1-x)^{-1/3}-1]\}$ versus $\ln\{[\text{NH}_3\text{H}_2\text{O}]/(\text{mol}\cdot\text{L})\}$, $\ln\{[(\text{NH}_4)_2\text{SO}_4]/(\text{mol}\cdot\text{L})\}$ and $\ln\{[\text{Na}_2\text{S}_2\text{O}_8]/(\text{mol}\cdot\text{L})\}$: (a) Ammonium; (b) Ammonium sulfate; (c) Sodium persulfate

ammonium sulfate and sodium persulfate were applied to developing the kinetics model. The rate constant of the new SCM model is directly proportional to the concentration of liquid reactant, and the effects of all the factors on the rate constant can be expressed as follows:

$$k=k_0[\text{NH}_3\text{H}_2\text{O}]^a\cdot[(\text{NH}_4)_2\text{SO}_4]^b\cdot[\text{Na}_2\text{S}_2\text{O}_8]^c\cdot e^{-E_a/(RT)} \quad (10)$$

Comparing Eq. (9) with Eq. (10), the dissolution kinetics of low-grade copper ore can be expressed as follows:

$$(1/3)\ln(1-x)+(1-x)^{-1/3}-1=k_0[\text{NH}_3\text{H}_2\text{O}]^a\cdot[(\text{NH}_4)_2\text{SO}_4]^b\cdot[\text{Na}_2\text{S}_2\text{O}_8]^c\cdot e^{-E_a/(RT)} \quad (11)$$

where k_0 is constant and E_a is the activation energy of the dissolution process. k_0 is calculated to be 53.46 min^{-1} according to the intercept of the straight lines in Fig. 9. Consequently, the following kinetics expression can be used to describe the dissolution of copper from the low-grade copper ore:

$$(1/3)\ln(1-x)+(1-x)^{-1/3}-1=53.46[\text{NH}_3\text{H}_2\text{O}]^{0.5}\cdot[(\text{NH}_4)_2\text{SO}_4]^{1.2}\cdot[\text{Na}_2\text{S}_2\text{O}_8]^{0.5}\cdot e^{-22910/(RT)} \quad (12)$$

4 Conclusions

1) The dissolution kinetics of copper from low-grade oxidized copper ore was investigated in ammonia-ammonium sulfate solution with sodium persulfate. It was found that agitation speed above 300 r/min is sufficient to eliminate the effect of agitation as a variable on the leaching rate. The extraction of copper is increased with the increase of reaction temperature, concentrations of ammonia, ammonium sulfate and sodium persulfate and with the decrease of particle size.

2) A new shrinking core model, which is based on the interfacial transfer and diffusion through the product layer, can be well used to describe the dissolution kinetics of copper in the ammonia- ammonium sulfate solution. The semi-empirical kinetics equation of the dissolution of copper can be expressed as Eq. (12). The activation energy was found to be 22.91 kJ/mol and the empirical reaction orders with respect to the concentrations of ammonia, ammonium sulfate and sodium persulfate were determined to be 0.5, 1.2 and 0.5, respectively.

3) The EDS and phase analyses of the residues indicate that malachite is dissolved completely, bornite is extracted by persulfate oxidation and chrysocolla can be partly dissolved in ammonia- ammonium sulfate solution.

References

- [1] ANTONIJEVIĆ M M, JANKOVIĆ Z D, DIMITRIJEVIĆ M D. Kinetics of chalcopyrite dissolution by hydrogen peroxide in

- sulphuric acid [J]. Hydrometallurgy, 2004, 71(3–4): 329–334.
- [2] WALTING H R. The bioleaching of sulphide minerals with emphasis on copper sulphide—A review [J]. Hydrometallurgy, 2006, 84(1–2): 81–108.
- [3] WU Heng-shan, LIU Yong. Study on copper recovery from tailing by means of leaching progress [J]. China Mining Magazine, 2001, 10(6): 65–67. (in Chinese)
- [4] ZHAO Guo-dong, WU Heng-shan, ZHANG Yu, LIU Qing. Ammonia leaching for tailings from a copper mine [J]. Nonferrous Metals, 2004, 56(3): 54–56. (in Chinese)
- [5] KÜNKÜL A, KOCAKERIM M M, YAPICI S, DEMIRBAĞ A. Leaching kinetics of malachite in ammonia solutions [J]. International Journal of Mineral Processing, 1994, 41(3–4): 167–182.
- [6] WANG Xi, CHEN Qi-yuan, HU Hui-ping, YIN Zhou-lan, XIAO Zhong-liang. Solubility prediction of malachite in aqueous ammoniacal ammonium chloride solutions at 25 °C [J]. Hydrometallurgy, 2009, 99(3–4): 231–237.
- [7] DEMIRKIRAN N, EKMEKYAPAR A, KÜNKÜL A, BAYSAR A. A kinetic study of copper cementation with zinc in aqueous solutions [J]. Inter J Miner Proc, 2007, 82(2): 80–85.
- [8] ÇALBAN T, ÇOLAK S, YEŞİLYURT M. Optimization of leaching of copper from oxidized copper ore in $\text{NH}_3\text{-(NH}_4)_2\text{SO}_4$ medium [J]. Chemical Engineering Communications, 2005, 192(10–12): 1515–1524.
- [9] BINGÖL D, CANBAZOĞLU M, AYDOĞAN S. Dissolution kinetics of malachite in ammonia/ammonium carbonate leaching [J]. Hydrometallurgy, 2005, 76(1–2): 55–62.
- [10] ARZUTUG M E, KOCAKERIM M M, COPUR M. Leaching of malachite ore in NH_3 -saturated water [J]. Ind Eng Chem Res, 2004, 43(15): 4118–4123.
- [11] EKMEKYAPAR A, OYA R, KÜNKÜL A. Dissolution kinetics of an oxidized copper ore in ammonium chloride solution [J]. Chem Biochem Eng Q, 2003, 17(4): 261–266.
- [12] LIU Wei, TANG Mo-tang, TANG Chao-bo. Dissolution kinetics of low grade complex copper ore in ammonia-ammonium chloride solution [J]. Transactions of Nonferrous Metals Society of China, 2010, 20(5): 910–917.
- [13] OUDENNE, P D, OLSON F A. Leaching kinetics of malachite in ammonium carbonate solutions [J]. Metallurgical Transactions B, 1983, 14(1): 33–40.
- [14] BINGÖL D, CANBAZOĞLU M. Dissolution kinetics of malachite in sulphuric acid [J]. Hydrometallurgy, 2004, 72(1–2): 159–165.
- [15] SOKIĆ M D, MARKIVIĆ B, ŽIVKOVIĆ D. Kinetics of chalcopryrite leaching by sodium nitrate in sulphuric acid [J]. Hydrometallurgy, 2009, 95(3–4): 273–279.
- [16] ADEBAYO A O, IPINMOROTI K O, AJAYI O O. Dissolution kinetics of chalcopryrite with hydrogen peroxide in sulphuric acid medium [J]. Chem Biochem Eng, 2003, 17(3): 213–218.
- [17] REILLY I G, SCOTT D S. The leaching of cupric sulfide in ammonia [J]. Ind Eng Chem Process Des Dev, 1976, 15(1): 60–67.
- [18] BELL S L, WELCH G D, BENNETT P G. Development of ammoniacal lixivants for the in-situ leaching of chalcopryrite [J]. Hydrometallurgy, 1995, 39(1–3): 11–23.
- [19] EKMEKYAPARS A, COLAK S, ALKAN M. Dissolution kinetics of an oxidized copper ore in water saturated by chlorine [J]. Journal of Chemical Technology and Biotechnology, 1988, 43(3): 195–204.
- [20] LI Dun-fang, WANG Cheng-yan, YIN Fei, CHEN Ying-qiang, JIE Xiao-wu. Effect of additive on copper removal from spent lithium-ion batteries by ammoniacal leaching [J]. Chinese Journal of Power Sources, 2009, 33(6): 454–457. (in Chinese)
- [21] REED W A, GARNOV Y A, RAO L, NASH K L, BOND A H. Oxidative alkaline leaching of Americium from simulated high-level nuclear waste sludges [J]. Separation Science and Technology, 2005, 40(5): 1029–1046.
- [22] PARK K H, MOHAPATRA D, REDDY B R, NAM C W. A study on the oxidative ammonia-ammonium sulfate leaching of a complex (Cu–Ni–Co–Fe) matte [J]. Hydrometallurgy, 2007, 86(3–4): 164–171.
- [23] FURMAN O S, TEEL A L, WATTS R J. Mechanism of base activation of persulfate [J]. Environment Science and Technology, 2010, 44(16): 6423–6428.
- [24] LEVENSPIEL O. Chemical reaction engineering [M]. New York: Wiley, 1972: 361–371.
- [25] DICKINSON C F, HEAL G R. Solid-liquid diffusion controlled rate equations [J]. Thermochimica Acta, 1999, 340–341: 89–103.

氨-硫酸铵体系过硫酸盐氧化含钙镁碳酸盐 低品位铜矿的浸出动力学

刘志雄^{1,2}, 尹周澜¹, 胡慧萍¹, 陈启元¹

1. 中南大学 化学化工学院, 长沙 410083;

2. 吉首大学 化学化工学院, 吉首 416000

摘要: 研究在氨-硫酸铵体系中用过硫酸盐氧化低品位铜矿浸出动力学, 确定搅拌速度、浸出温度、矿物粒度及氨、硫酸铵和过硫酸钠的浓度对浸出的影响。结果表明, 搅拌速度在 300 r/min 以上时对浸出速度无影响, 浸出速度随反应温度及氨、硫酸铵和过硫酸钠浓度的增大而增加。对浸出渣的 EDS 和物相定量分析表明斑铜矿被过硫酸盐氧化而溶解于氨-硫酸铵溶液。用产物层的界面传质和扩散控制的收缩核模型分析铜矿的溶解动力学, 其表观活化能为 22.91 kJ/mol, 同时获得了描述浸出过程的半经验动力学方程, 其对氨、硫酸铵和过硫酸钠的浓度的表观反应级数分别为 0.5、1.2 和 0.5。

关键词: 低品位复杂铜矿; 钙-镁碳酸盐; 氧化浸出; 浸出动力学; 氨-硫酸铵; 过硫酸钠; 活化能; 收缩核模型

(Edited by LI Xiang-qun)